

Rare-earth intermetallic compounds at a magnetic instability

H.v. Löhneysen^{a,b,*}, H. Bartolf^a, S. Drotziger^a, C. Pfleiderer^{a,b,1},
O. Stockert^c, D. Souptel^d, W. Löser^d, G. Behr^d

^a *Physikalisches Institut, Universität Karlsruhe, D-76128 Karlsruhe, Germany*

^b *Institut für Festkörperphysik, Forschungszentrum Karlsruhe, D-76021 Karlsruhe, Germany*

^c *Max-Planck-Institut für chemische Physik fester Stoffe, D-01187 Dresden, Germany*

^d *Institut für Festkörper- und Werkstoffforschung, D-01069 Dresden, Germany*

Available online 14 July 2005

Abstract

Rare-earth intermetallic alloys and compounds, in particular those with Ce or Yb, are often close to a magnetic instability. In particular, CeCu_{6-x}Au_x has become a prototype heavy-fermion (HF) system where, starting from not magnetically ordered CeCu₆, Au doping introduces long-range incommensurate antiferromagnetism for $x > x_c \approx 0.1$. At the critical concentration x_c the system experiences a quantum phase transition (QPT). Here, the unusual magnetic fluctuations probed by inelastic neutron scattering lead to non-Fermi-liquid behavior, i.e. to anomalous low-temperature thermodynamic and transport properties. Hall-effect measurements delineate the “bandstructure” of heavy fermions across the critical concentration x_c . While most rare-earth HF compounds have a tendency towards antiferromagnetic order, CeSi_{1.81} presents one of the comparatively few cases exhibiting ferromagnetic order below $T_c = 9.5$ K. In a search for a ferromagnetic QPT in HF metals, we have studied the pressure dependence of the magnetization and the spontaneously ordered magnetic moment, μ_S , which vanishes around $p \approx 13$ kbar.

© 2005 Elsevier B.V. All rights reserved.

PACS: 75.30.Mb; 71.27.+a; 71.10.Hf; 75.20.Hr; 75.40.Gb

Keywords: Rare-earth; Magnetic instability; Non-Fermi-liquid behavior

1. Introduction

In many rare-earth intermetallic compounds and alloys, the strength of the conduction-electron–f-electron exchange interaction, J , can be tuned by composition or pressure, giving rise to either dominant Kondo or RKKY interactions [1]. This leads to heavy-fermion (HF) behavior when the energy scale of the Kondo interaction is slightly larger than that of the RKKY interaction, and offers the possibility to induce a zero-temperature magnetic–nonmagnetic transition.

CeCu_{6-x}Au_x has become a prototype HF system where, starting from not magnetically ordered CeCu₆ with strongly

enhanced Pauli paramagnetism, Au doping introduces long-range incommensurate antiferromagnetism for Au concentration $x > x_c \approx 0.1$ [2]. This transition arises because the exchange interaction, J , can be tuned by composition, by virtue of the negative lattice expansion caused by the large Au radius [3]. Indeed, the long-range magnetic order can be suppressed by applying hydrostatic pressure, p [4,5]. Hence, composition and pressure can be employed to tune the delicate balance between dominant Kondo or RKKY interactions. Of course, for an anisotropic system such as CeCu_{6-x}Au_x with the orthorhombic Pnma structure, anisotropy effects in the x or p dependence of the lattice parameters have to be taken into account. In addition, a small monoclinic distortion ($<1.5^\circ$) occurs for $x < 0.14$ [2]. (For simplicity, we always use the orthorhombic unit cell to denote the crystallographic directions.) A detailed study of this transition by means of thermal expansion measurements has shown that it is not related

* Corresponding author. Tel.: +49 721 608 3450; fax: +49 721 608 6103.

E-mail address: h.vl@phys.uni-karlsruhe.de (H.v. Löhneysen).

¹ Present address: Physik Department E21, Technische Universität München, D-85748 Garching, Germany.

to the magnetic instability [6]. A magnetic instability as in $\text{CeCu}_{6-x}\text{Au}_x$, which can ideally be traced to absolute zero temperature, offers the possibility of studying a magnetic quantum phase transition. In the vicinity of this transition, non-Fermi-liquid (NFL) behavior manifests itself as a strong deviation of thermodynamic and transport properties from Fermi-liquid (FL) predictions. For $\text{CeCu}_{5.9}\text{Au}_{0.1}$, the linear specific-heat coefficient $\gamma = C/T$ acquires an unusual temperature dependence, $\gamma \sim -\ln(T/T_0)$, and the T -dependent part of the electrical resistivity $\Delta\rho = \rho - \rho_0$, where ρ_0 is the residual resistivity, varies as $\Delta\rho \sim T^m$, with $m \approx 1$ [2,7].

In the spin-density-wave scenario, the NFL behavior observed in HF systems at the magnetic–nonmagnetic transition arises from a proliferation of low-energy magnetic excitations [8–10]. This transition, being induced by an external parameter such as concentration or pressure, as mentioned above, may in principle occur at $T = 0$. If the transition is continuous, it is driven by quantum fluctuations instead of thermal fluctuations in finite- T transitions. The critical behavior of such a quantum phase transition (QPT) at $T = 0$ is governed by the spatial dimension d of incipient magnetic order and the dynamical exponent z . For three spatial dimensions, the renormalization-group treatment by Millis [9] essentially corroborates the previous predictions of the self-consistent renormalization (SCR) theory of spin fluctuations [10]. The case of 2D antiferromagnetic fluctuations (i.e. $d = 2, z = 2$) coupled to itinerant quasiparticles with 3D dynamics has been worked out by Rosch and co-workers [11]. The NFL features observed in $\text{CeCu}_{6-x}\text{Au}_x$, i.e. $C/T \sim -\ln(T/T_0)$ and $\Delta\rho \sim T$, can be nicely explained by this scenario. Indeed, inelastic neutron scattering (INS) experiments performed on a $x = 0.1$ single crystal over a wide range in reciprocal space revealed a strong spatial anisotropy of the critical magnetic fluctuations, thus suggesting the presence of quasi 2D fluctuations [12].

On the other hand, a detailed study of the energy and temperature dependence of the fluctuations carried out by Schröder et al. [13,14] demonstrated convincingly E/T scaling of the dynamic susceptibility, indicating that taking the Hertz–Millis theory at face value, one is in fact below the upper critical dimension. Even more, the E/T scaling comes with an anomalous scaling exponent $\alpha = 0.75$ that is distinctly different from the Lorentzian response ($\alpha = 1$). In addition, this highly unusual E/T scaling (observed earlier – with a different value of α – for another NFL system, i.e. $\text{UCu}_{5-x}\text{Pd}_x$ [15]) appears everywhere in the Brillouin zone, and $\alpha = 0.8$ is even observed for the T dependence of the static uniform susceptibility (i.e. $E = 0, q = 0$) [13,14]. This implies that the dynamics of the critical fluctuations is local, prompting Coleman et al. [14,16] to suggest that one is witnessing a more drastic variant of non-Fermi-liquid behavior than in the Hertz–Millis scenario applied to HF systems. The local criticality might signal that the heavy quasiparticles themselves, being composite objects arising from the conduction electron– f -electron interaction, disintegrate [14,16]. Therefore, one might expect that the Kondo temperature, T_K , being a measure of the binding energy of

the quasiparticles, goes to zero at the quantum critical point (QCP). In a model of a locally critical QPT, a “destruction” of the Kondo resonance has been suggested which leads to critical local-moment fluctuations [17,18]. Hall-effect measurements have been suggested to distinguish between Hertz–Millis and Coleman–Si scenarios [16].

Weak residual interactions might break the delicate balance between quantum liquid (Fermi liquid) and quantum solid (magnetic order) at the QCP. For instance, there is increasing evidence for magnetic ordering in CeCu_6 occurring around 2 mK [19]. The presence of a corresponding (very small) energy scale of course renders quantum fluctuations irrelevant below that energy. In the present work, focusing on experiments at higher temperatures ($T_{\min} \approx 20$ mK), we will neglect this low-energy scale.

While the competition between Kondo and RKKY interactions leads to antiferromagnetic order for the large majority of rare-earth compounds, a few examples of ferromagnetic Ce compounds or alloys exist [20]. Here, we present measurements of ferromagnetic $\text{CeSi}_{1.81}$ [21] under pressure, where the spontaneously ordered moment and the Curie temperature can be driven to absolute zero around 13 kbar. Previous experiments on polycrystalline CeSi_x samples did not give a clear dependence of the ferromagnetic ordering under pressure [22].

In this paper, we will discuss recent experiments on $\text{CeCu}_{6-x}\text{Au}_x$ in the vicinity of x_c , i.e. $0 \leq x \leq 0.3$ which address the following issues: (i) evolution of the ordered moment with x , (ii) exploration of the fluctuations away from the critical concentration $x_c \approx 0.1$, (iii) first measurements of the Hall constant across x_c . We will also discuss magnetization measurements on $\text{CeSi}_{1.81}$ under pressure.

2. Ordered moments, magnetic fluctuations, Hall effect and coherence maximum across the critical concentration in $\text{CeCu}_{6-x}\text{Au}_x$

The occurrence of antiferromagnetic order in $\text{CeCu}_{6-x}\text{Au}_x$ beyond a threshold concentration $x_c \approx 0.1$ was inferred early on from sharp maxima in the specific heat and low-field

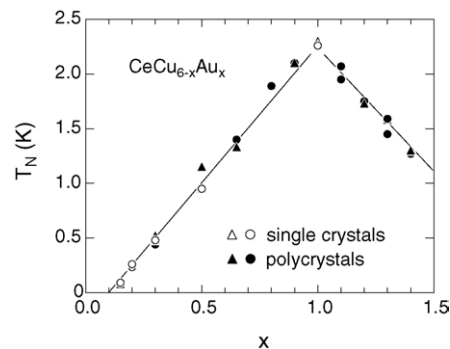


Fig. 1. Dependence of the Néel temperature T_N of $\text{CeCu}_{6-x}\text{Au}_x$ on Au concentration x . T_N varies linearly between $x = x_c \approx 0.1$ and $x = 1$.

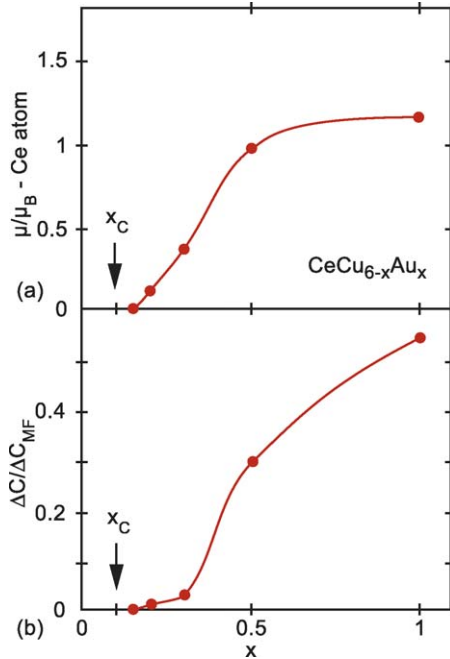


Fig. 2. (a) Ordered magnetic moment of antiferromagnetic $\text{CeCu}_{6-x}\text{Au}_x$ as a function of x as determined from elastic neutron scattering. (b) Magnitude of the specific-heat anomaly ΔC at T_N , giving a measure of the ordered moment in a spin-density-wave scenario. ΔC is normalized to the value $\Delta C_{\text{MF}} = 1.5R$ for an effective $s = \frac{1}{2}$ system.

dc magnetization [23,24]. For $x > 0.1$ the Néel temperature T_N varies linearly with x up to $x = 1$, where the stoichiometric compound CeCu_5Au is formed, with the Au atoms completely and exclusively occupying the Cu(2) site of the CeCu_6 structure [25] (see Fig. 1).

The magnetic structure of $\text{CeCu}_{6-x}\text{Au}_x$ was determined for various concentrations between $x = 0.15$ and 1 by elastic neutron scattering [26]. For $x \leq 0.4$, the Q vector of the incommensurate structure lies in the a^*c^* plane, e.g. $Q = (0.625\ 0\ 0.275)$ for $x = 0.2$, and hardly depends on x [26,27]. However, for $x \geq 0.5$ incommensurate order is

observed along the a^* axis, with $Q = (0.59\ 0\ 0)$. Assuming a sinusoidal modulation of the magnetic moments, aligned along the easy c axis, we can estimate an average ordered moment of $0.1\text{--}0.15\ \mu_B/\text{Ce atom}$ for $x = 0.2$, and $0.3\text{--}0.45$ for $x = 0.3$. For $x = 0.5$ and 1, $\mu \approx 1.0$ and $1.15\ \mu_B/\text{Ce atom}$, respectively, is estimated [26]. The variation of $\mu(x)$ as shown in Fig. 2(a) and the change of Q between $x = 0.4$ and 0.5 is contrasted in a remarkable fashion by the simple linear $T_N(x)$ dependence, which appears not to be affected by either of these features. The 3D ordering Bragg peaks for $x = 0.15, 0.2$ and 0.3 are all located in the q -space region of the anisotropic fluctuations for $x = 0.1$ [26] which therefore can be viewed as precursors of 3D ordering.

What happens to the critical fluctuations if one moves away from the critical concentration x_c ? The investigation of magnetic fluctuations in CeCu_6 , i.e. not too far from the QCP, has in fact a long history [28,29]. Fig. 3 shows scans along the c^* direction in the reciprocal a^*c^* plane for $x = 0$, and 0.2 as measured with an energy transfer of $\hbar\omega = 0.15\ \text{meV}$, together with the data for the critical concentration $x = 0.1$ ($\hbar\omega = 0.1\ \text{meV}$) for comparison.

An important observation is that the peculiar q dependence of the fluctuations, nicknamed “rods” [12] or “butterfly” [14] persists to $x = 0.2$ as well as to $x = 0$ (see Fig. 4, where a grey-scale figure of the data of Fig. 3 are shown). We note that the present data for CeCu_6 have been taken with much higher resolution than the previous data [28,29]. Apparently, therefore, the double-maximum feature along a^* , i.e. in $(h\ 0\ 0)$ scans (not shown), could not be resolved in the early work. However, all data are compatible with each other, taking the difference in resolution into account. The fact that the “rod/butterfly” structure of critical fluctuations in $\text{CeCu}_{5.9}\text{Au}_{0.1}$ is present in pure CeCu_6 as well, rules out disorder as an origin of this remarkable feature of the quantum phase transition in $\text{CeCu}_{6-x}\text{Au}_x$. That disorder does not qualitatively affect the QPT had already been inferred from the fact that pressure tuning the Néel temperature to zero for $x = 0.2$ and 0.3 leads to

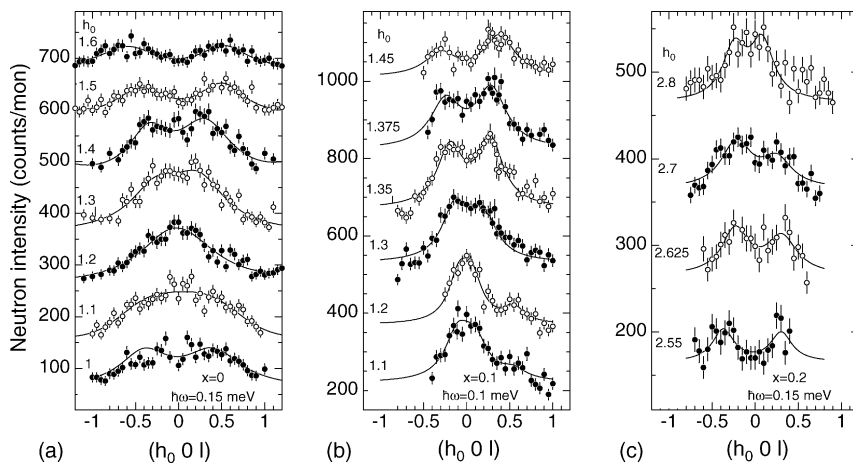


Fig. 3. Inelastic neutron scattering scans in the reciprocal a^*c^* plane of $\text{CeCu}_{6-x}\text{Au}_x$ for (a) $x = 0$, energy transfer $\hbar\omega = 0.15\ \text{meV}$, (b) $x = 0.1$, $\hbar\omega = 0.10\ \text{meV}$ and (c) $x = 0.2$, $\hbar\omega = 0.15\ \text{meV}$. Data were taken at the triple axis spectrometer IN 12 at the ILL Grenoble.

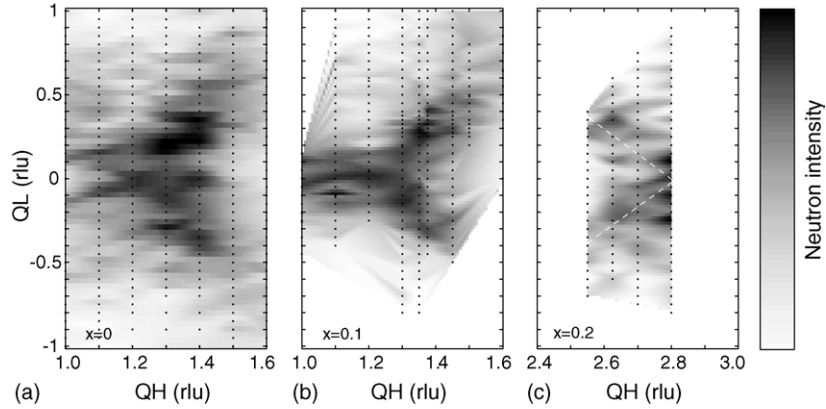


Fig. 4. Grey-scale contours of inelastic neutron scattering intensity in the a^*c^* plane for the data of Fig. 3(a–c).

the same specific-heat behavior $C/T = a \ln(T_0/T)$ at the critical pressure, p_c , of about 4 and 8 kbar, respectively, with identical (within the accuracy of measurement) coefficients a and T_0 [3].

The concentration dependence of the ordered moment, μ , of $\text{CeCu}_{6-x}\text{Au}_x$ as determined from the elastic neutron-scattering data already reported above (Fig. 2(a)) [26] is compared with the size of the specific-heat anomaly at T_N which may be related to μ . Assuming a mean-field-like jump ΔC normalized to $\Delta C_{\text{MF}} = 1.5 R$ expected for a fully ordered of effective spin $s = 1/2$, [25], a direct comparison within the spin-density-wave scenario is possible. Both data are qualitatively consistent with each other, although the onset of ordered moment inferred from ΔC just above x_c is much slower, possibly because of short-range-order effects smearing the transition. In any case, both data sets are clearly inconsistent with the behavior $\mu \sim |x - x_c|^{3/4}$ predicted by the 3D Hertz–Millis scenario.

In order to shed more light on the fate of the heavy Fermi liquid across x_c , we have started to investigate the Hall effect. Fig. 5 shows data of the Hall constant $R_H(T)$ for various x , measured in $B = 1$ T applied along the easy direction (c axis). The choice of this field was such that one is always outside the antiferromagnetically ordered state which for $x = 0.2$ is suppressed for $B \geq 0.42$ T [30]. The current flow was parallel to the a axis unless stated otherwise. Previous data for $x = 0$ [31,32] and 0.1 [32] are in good agreement with our data in the region of overlap. For $300 \text{ K} \gtrsim T \gtrsim 20 \text{ K}$, R_H is nearly independent of x and shows with decreasing T a smooth evolution from negative to positive R_H . Below 10 K, a strong x dependence is observed. R_H for the $x = 0$ sample passes over a shallow maximum near 15 K and undergoes a second sign change with decreasing T , passes over a minimum and finally acquires a constant negative value $R_H(0)$ for $T \lesssim 70$ mK. Already for $x = 0.05$, R_H becomes slightly positive at low T , and again is independent of T (here actually between 4 K and 25 mK). For $x = 0.1, 0.15$ and 0.2 , $R_H(T)$ rises strongly towards positive values between 10 and 0.2 K, and a coherent groundstate with $R_H = R_H(0)$ independent of T is reached below ~ 100 mK. The data can be interpreted in two different

ways. Taken at face value, the sign change of $R_H(0)$ suggests a transition from a hole-like to an electron-like Fermi surface being due to the complex bandstructure of the heavy quasiparticles in CeCu_6 . On the other hand, R_H is in fact composed of two contributions, the normal (n) and anomalous (a) Hall constant R_H^n and R_H^a . R_H^a arises from skew scattering off magnetic moments. A detailed analysis is in progress. Using the free-electron formula $R_H = 1/ne$ we obtain an effective conduction-electron concentration $n = -0.73/\text{f.u.}$ for $x = 0$ and $n = +0.061/\text{f.u.}$ for $x = 0.2$, corresponding to a change of ~ 0.8 across the QPT. This large change of n appears not to be compatible with the rather small evolving ordered moment that in a spin-density-wave scenario would “drop out” of the Fermi sea. However, lacking a detailed bandstructure calculation of CeCu_6 and a detailed analysis of the Hall effect, a definite conclusion would be premature.

The Kondo temperature, T_K , is well defined for a single isolated magnetic impurity in a metallic host only. It is well known that in HF systems such as CeCu_6 which can in certain aspects be viewed as a Kondo lattice, T_K will be renormalized because of the interactions between Kondo “impurities”. Here, we adopt the pragmatic point of view that T_K in a HF system presents the self-consistently determined mean binding energy of the heavy quasiparticles. Well below T_K , in a lattice with translational symmetry, these quasiparticles will be eigenstates of the periodic potential, strongly modified by

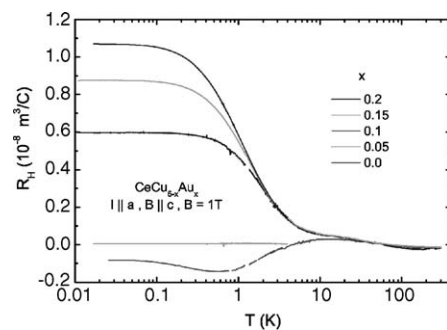


Fig. 5. Hall constant R_H of $\text{CeCu}_{6-x}\text{Au}_x$ as a function of T , measured in a field of $B = 1$ T applied along the easy c direction.

electron-electron interactions. This gives rise to a maximum ρ_{\max} of the resistivity $\rho(T)$ in many HF systems, signaling the onset of lattice coherence of the quasiparticles and finally, to the FL T^2 dependence of ρ . The temperature of the coherence maximum is therefore usually called coherence temperature T_{coh} . The specific heat of $\text{La}_{1-y}\text{Ce}_y\text{Cu}_6$ scales with the Ce concentration y , indicating a simple superposition of individual Kondo-impurity contributions [33], although one has to bear in mind that there are numerous counter examples where such a scaling does not hold. T_K can be tuned by hydrostatic pressure because it depends sensitively on J , $T_K \sim \exp(-1/N(E_F)J)$, where $N(E_F)$ is the (unrenormalized) conduction-electron density of states at the Fermi level. For CeCu_6 , the electrical resistivity, normalized to its value ρ_{\max} under pressure, scales reasonably well with T/T_{coh} over a wide range of T and p [34], implying the presence of an intimate relation between T_{coh} and T_K . A recent analysis of $\text{Ce}_x\text{La}_{1-x}\text{CoIn}_5$ suggests a phenomenological two-fluid model for a Kondo lattice [35]. We therefore argue that the very presence of a coherence maximum in $\text{CeCu}_{6-x}\text{Au}_x$ implies the existence of a finite Kondo energy scale. This qualitative assessment is independent of exactly how the Kondo temperature depends on x or p and therefore much more robust than an attempt to quantitatively evaluate T_K .

Shown in Fig. 6(a) is the resistivity $\rho(T/T_{\max})/\rho_{\max}$ for different x . Here, T_{\max} is the temperature where the maximum ρ_{\max} occurs. For $0 \leq x \leq 0.15$, a resistance maximum is clearly resolved. The resistivity maximum presents a crossover which, when considering different alloys, is also affected by the magnitude of the residual resistivity ρ_0 and disorder scattering, which of course strongly depends on x . It is thus denoted by T_{\max} and not by T_{coh} . We therefore do not expect a scaling of $\rho(T/T_{\max})/\rho_{\max}$ as seen in CeCu_6 under pressure [34]. In addition, the onset of magnetic order, with its pronounced effect on transport [26], precludes the observation of a maximum for $x > 0.2$. For $x = 0.2$, an upper bound can be given by $T_{\max} < T_N$, leading to the position of the $x = 0.2$ data as indicated in Fig. 6(a). T_{\max} versus x is shown in Fig. 6(b). The main point to note is the smooth, nearly linear decrease of T_{\max} which appears to vanish at $x \approx 0.16$. In particular, no anomaly of $T_{\max}(x)$ occurs in the vicinity of the QCP at $x = 0.1$. We conclude that because T_{\max} remains finite, a fortiori T_K must remain finite as well, whatever the exact relation between T_{\max} and the binding energy of quasiparticles may be. Hence, it appears that the local energy scale which has been suggested to vanish in recently proposed scenarios [14,16] of the QPT in $\text{CeCu}_{6-x}\text{Au}_x$, is not directly related to T_K .

3. Suppression of ferromagnetism in $\text{CeSi}_{1.81}$ by hydrostatic pressure

CeSi_x crystallizes for $x \lesssim 1.85$ in the orthorhombic α - GdSi_2 structure (Imma) and for $x \gtrsim 1.85$ in the tetragonal α - ThSi_2 structure ($I4_1/amd$) [36]. In both cases, of course,

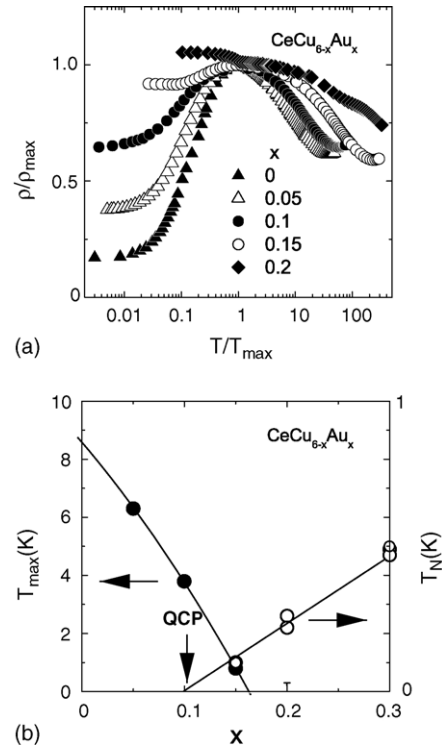


Fig. 6. (a) Electrical resistivity ρ/ρ_{\max} of $\text{CeCu}_{6-x}\text{Au}_x$ vs. $T/T_{\max} \cdot \rho_{\max}$ and T_{\max} denote the $\rho(T)$ maximum. (b) T_{\max} (left scale) and T_N (right scale) vs. x . Vertical bar denotes upper limit of T_{\max} for $x = 0.2$.

the Si deficiency leads to Si vacancies. This phase diagram, differing somewhat from previous studies [21,37], suggests that the orthorhombic-tetragonal transition as a function of x coincides with the ferromagnetic-paramagnetic transition. Ferromagnetism had been reported earlier for samples in the range $x \lesssim 1.80$ [21]. The samples of the present study were prepared by arc melting polycrystalline ignots followed by zone-refining to obtain single crystals. This procedure yields single-phase crystals only in the narrow concentration range $1.81 < x < 1.82$. For larger x , small Si precipitates were found. Here, we focus on a crystal with $x = 1.81$ which had been characterized previously [36].

Fig. 7 shows ferromagnetic hysteresis loops $M(B)$ for different temperatures. Here and in the following, the field was always applied to the easy direction (a axis). The hysteresis loop taken at the lowest temperature 1.6 K shows some step-like structure which might be interpreted as arising from two different Ce sites exhibiting different coercive fields or, alternatively, from two different ferromagnetic sublattices coupled by a very weak antiferromagnetic or canting interaction. At 5.1 K, the hysteresis loop has become considerably narrower and the step-like structure has vanished. At 10 K, the system is always in the paramagnetic state. Fig. 8 shows magnetization data for $M(B)$ for magnetic fields up to 12 T. The data were always taken by sweeping the applied magnetic field B from initially -0.5 T upwards, i.e. starting on the lower branch of the hysteresis loop. Below about 5 K, a hump in $M(B)$ around 4 T is clearly visible indicating again,

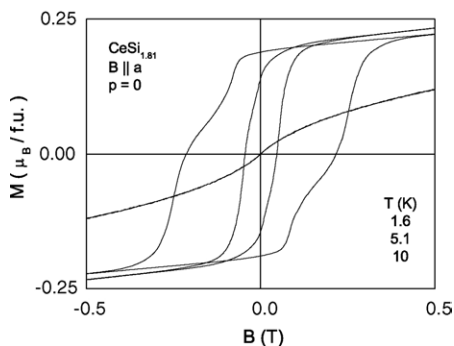


Fig. 7. Magnetic hysteresis loops $M(B)$ of $\text{CeSi}_{1.81}$ with the field applied parallel to the easy a direction for three different temperatures: $T = 1.6$ K (wide loop), $T = 5.1$ K (narrow loop), $T = 10$ K (no hysteresis).

like the step-like feature in the hysteresis loops, that the low- T ferromagnetic order is in fact more complicated. Looking at both figures, it is also apparent that the spontaneously ordered moment, μ_S , obtained by extrapolating the magnetization curves to $B = 0$, passes over a shallow maximum around 4 K (Fig. 9). μ_S vanishes at $T_c = 9.5$ K in a continuous fashion, signaling a second-order transition from ferromagnet to paramagnet. The spontaneous moment μ_S is much smaller than the effective moment determined from the low-field susceptibility above T_c , $\mu_{\text{eff}} = 2.05\mu_B/\text{f.u.}$ μ_{eff} is somewhat reduced compared to the Ce^{3+} free-ion value of $2.54\mu_B/\text{f.u.}$ which probably is due to crystal-field effects. Furthermore, the magnetization shows no sign of saturation up to 12 T. This feature and the fact that $\mu_S/\mu_{\text{eff}} \ll 1$ indicate that we are dealing with a weak itinerant ferromagnet.

Finally, Fig. 10 shows the spontaneous moment for various hydrostatic pressures p . μ_S is gradually suppressed with increasing p and vanishes around $p_c \approx 13$ kbar. Likewise, $T_c(p)$ vanishes around the same pressure (not shown). Since the data were taken above 2.3 K, an extension of the measurements to $T < 1$ K is necessary to determine the functional $T_c(p)$ dependence for $T_c \rightarrow 0$. The $M(B)$ data under pressure show further interesting features to be reported in detail elsewhere [40]. (i) The hump in $M(B)$ disappears above $p \sim 5$ kbar and $\mu_S(p)$ shows a shallow maximum at that pressure, in loose analogy to the temperature dependence of the

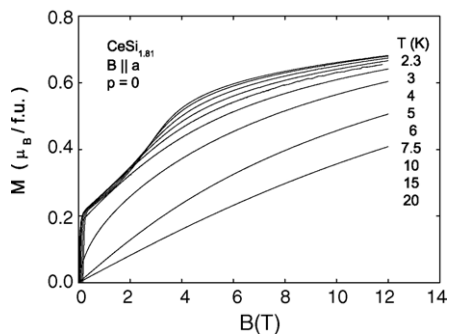


Fig. 8. Magnetization M of $\text{CeSi}_{1.81}$ as a function of applied field B at ambient pressure $p = 0$ for different temperatures T , increasing from top to bottom.

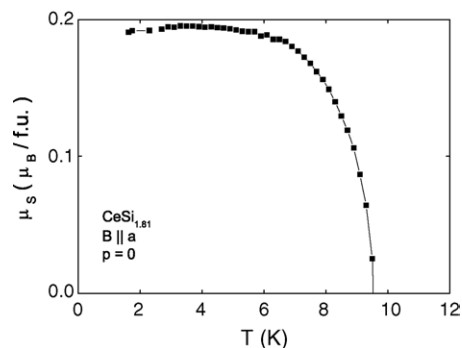


Fig. 9. Spontaneous moment μ_S as a function of temperature T for $p = 0$.

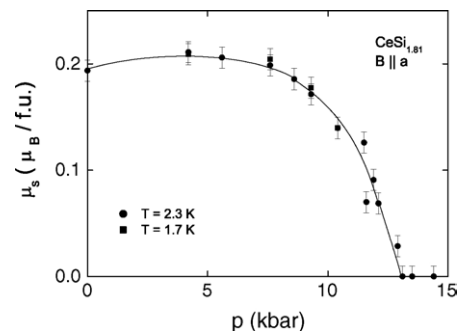


Fig. 10. Spontaneous moment μ_S as a function of hydrostatic pressure p measured at $T = 1.7$ and 2.3 K.

$M(B)$ curves. (ii) The slope of $M(B)$ is independent of p , even for small applied fields. This may suggest that the low-field susceptibility remains finite when approaching the critical pressure p_c . However, measurements to lower temperatures have to be carried out. Furthermore, the origin of the unusual $M(B)$ and hysteresis loops has to be determined. In addition, domain-structure effects have to be taken into account.

4. Conclusion

Although the quantum phase transition in $\text{CeCu}_{6-x}\text{Au}_x$ has been studied for ten years, new features evolve continuously as this prototype system is probed in depth. The existence of the complex dependence of the magnetic fluctuations finds its expression in precursor effects with the same q dependence in pure CeCu_6 , showing that disorder is not relevant for this feature. Likewise, the search for a relevant local low-energy scale that vanishes at the QCP must be continued. Finally, an all-important issue is whether the physics of $\text{CeCu}_{6-x}\text{Au}_x$ presents a singular case, or whether it is a representative of a more general behavior akin to strongly correlated electron systems at a QCP. Certainly, there are HF systems that follow a more conventional spin-density-wave scenario, as $\text{Ce}_{1-x}\text{La}_x\text{Ru}_2\text{Si}_2$ [38], while thermodynamic and transport measurements on YbRh_2Si_2 show very unusual features [39] with some similarities, but also distinct differences to $\text{CeCu}_{6-x}\text{Au}_x$, that remain to be understood. Therefore,

the search for new systems exhibiting quantum criticality, and their thorough investigation, is a challenging task for the future. The investigation of ferromagnetic CeSi_{1.81} reported here is a first step in this direction.

Acknowledgements

The inelastic neutron scattering experiments were carried out at the Institut Laue-Langevin Grenoble. We are grateful for the possibility to perform these experiments and for technical support. We thank the Deutsche Forschungsgemeinschaft and the Helmholtz-Gemeinschaft (HGF) for financial support.

References

- [1] S. Doniach, *Physica B* 91 (1977) 213.
- [2] H.v. Löhneysen, A. Schröder, O. Stockert, *J. Alloys Compd.* 303–304 (2000) 480.
- [3] H.v. Löhneysen, *J. Magn. Magn. Mater.* 200 (1999) 532.
- [4] A. Germann, H.v. Löhneysen, *Europhys. Lett.* 9 (1989) 367.
- [5] B. Bogenberger, H.v. Löhneysen, *Phys. Rev. Lett.* 74 (1995) 1916.
- [6] K. Grube, W.H. Fietz, U. Tutsch, O. Stockert, H.v. Löhneysen, *Phys. Rev. B* 60 (1999) 11947.
- [7] H.v. Löhneysen, T. Pietrus, G. Portisch, H.G. Schlager, A. Schröder, M. Sieck, T. Trappmann, *Phys. Rev. Lett.* 72 (1994) 3262.
- [8] J.A. Hertz, *Phys. Rev. B* 14 (1976) 1165.
- [9] A.J. Millis, *Phys. Rev. B* 48 (1993) 7293.
- [10] T. Moriya, T. Takimoto, *J. Phys. Soc. Jpn.* 64 (1995) 960 (and references therein).
- [11] A. Rosch, A. Schröder, O. Stockert, H.v. Löhneysen, *Phys. Rev. Lett.* 79 (1997) 150.
- [12] O. Stockert, H.v. Löhneysen, A. Rosch, N. Pyka, M. Loewenhaupt, *Phys. Rev. Lett.* 80 (1998) 5627.
- [13] A. Schröder, G. Aeppli, E. Bucher, R. Ramazashvili, P. Coleman, *Phys. Rev. Lett.* 80 (1998) 5623.
- [14] A. Schröder, G. Aeppli, R. Coldea, M. Adams, O. Stockert, H.v. Löhneysen, E. Bucher, R. Ramazashvili, P. Coleman, *Nature* 407 (2000) 351.
- [15] M.C. Aronson, R. Osborn, R.A. Robinson, J.W. Lynn, R. Chau, C.L. Seaman, M.B. Maple, *Phys. Rev. Lett.* 75 (1995) 725.
- [16] P. Coleman, C. Pépin, Q. Si, R. Ramazashvili, *J. Phys. Condens. Matter* 13 (2001) 723.
- [17] Q. Si, S. Rabello, K. Ingersent, J.L. Smith, *Nature* 413 (2000) 804.
- [18] K. Ingersent, Q. Si, *Phys. Rev. B* 89 (2002) 076403.
- [19] H. Tsujii, E. Tanaka, Y. Ode, T. Katoh, T. Mamiya, S. Araki, R. Settai, Y. Ōnuki, *Phys. Rev. Lett.* 84 (2000) 5407.
- [20] J. Sereni, K.A. Geschneidner Jr., L. Eyring (Eds.), *Handbook of Physics and Chemistry of Rare Earths*, vol. 15, Elsevier, 1991, p. 1.
- [21] H. Yashima, H. Mori, T. Satoh, *Solid State Commun.* 43 (1982) 193.
- [22] S.A. Shaheen, J.S. Schilling, *Phys. Rev. B* 35 (1987) 6880.
- [23] A. Germann, A.K. Nigam, J. Dutzi, A. Schröder, H.v. Löhneysen, *J. Phys. Coll.* 49 (1988) C8–C755.
- [24] H.G. Schlager, A. Schröder, M. Welsch, H.v. Löhneysen, *J. Low Temp. Phys.* 90 (1993) 181.
- [25] M. Ruck, G. Portisch, H.G. Schlager, M. Sieck, H.v. Löhneysen, *Acta Cryst. Sect. B* 49 (1993) 936.
- [26] H.v. Löhneysen, A. Neubert, T. Pietrus, A. Schröder, O. Stockert, U. Tutsch, M. Loewenhaupt, A. Rosch, P. Wölfle, *Eur. Phys. J. B* 5 (1998) 447 (and references therein).
- [27] H. Okumura, K. Kakurai, Y. Yoshida, Y. Ōnuki, Y. Endoh, *J. Magn. Magn. Mater.* 177–181 (1998) 405.
- [28] G. Aeppli, H. Yoshizawa, Y. Endoh, E. Bucher, J. Hufnagl, Y. Ōnuki, T. Komatsubara, *Phys. Rev. Lett.* 57 (1986) 122.
- [29] J. Rossat-Mignod, L.P. Regnault, J.L. Jacoud, C. Vettier, P. Lejay, J. Flouquet, E. Walker, D. Jaccard, A. Amato, *J. Magn. Magn. Mater.* 76–77 (1988) 376.
- [30] H.v. Löhneysen, C. Pfeleiderer, T. Pietrus, O. Stockert, B. Will, *Phys. Rev. B* 63 (2001) 134411.
- [31] F. Milliken, T. Penney, F. Holtzberg, Z. Fisk, *J. Magn. Magn. Mater.* 76–77 (1988) 201.
- [32] T. Namiki, H. Sato, J. Urakawa, H. Sugawara, Y. Aoki, R. Settai, Y. Ōnuki, *Physica B* 281–282 (2000) 359.
- [33] Y. Ōnuki, T. Komatsubara, *J. Magn. Magn. Mater.* 63–64 (1987) 281.
- [34] S. Yomo, L. Gao, R.L. Meng, P.H. Hor, C.W. Chu, J. Susaki, *J. Magn. Magn. Mater.* 76–77 (1988) 257.
- [35] S. Nakatsuji, D. Pines, Z. Fisk, *Phys. Rev. Lett.* 92 (2004) 016401.
- [36] D. Souptel, G. Behr, W. Löser, A. Teresiak, S. Drotziger, C. Pfeleiderer, *J. Cryst. Growth* 269 (2004) 606.
- [37] W.H. Lee, R.N. Shelton, S.K. Dhar, K.A. Geschneidner Jr., *Phys. Rev. B* 35 (1987) 8523.
- [38] W. Knafo, S. Raymond, J. Flouquet, B. Fåk, M.A. Adams, P. Haen, F. Lapiere, S. Yates, P. Lejay, *Phys. Rev. B* 70 (2004) 174401.
- [39] J. Custers, P. Gegenwart, H. Wilhelm, K. Neumaier, Y. Tokiwa, O. Trovarelli, C. Geibel, F. Steglich, C. Pépin, P. Coleman, *Nature* 424 (2003) 524.
- [40] S. Drotziger, C. Pfeleiderer, H.v. Löhneysen, D. Souptel, W. Löser, G. Behr, *Physica B* 359–361 (2005) 92.